



National Library
of Canada

Bibliothèque nationale
du Canada

Canadian Theses Service

Services des thèses canadiennes

Ottawa, Canada
K1A 0N4

CANADIAN THESES

THÈSES CANADIENNES

NOTICE

The quality of this microfiche is heavily dependent upon the quality of the original thesis submitted for microfilming. Every effort has been made to ensure the highest quality of reproduction possible.

If pages are missing, contact the university which granted the degree.

Some pages may have indistinct print, especially if the original pages were typed with a poor typewriter ribbon or if the university sent us an inferior photocopy.

Previously copyrighted materials (journal articles, published tests, etc.) are not filmed.

Reproduction in full or in part of this film is governed by the Canadian Copyright Act, R.S.C. 1970, c. C-30.

THIS DISSERTATION
HAS BEEN MICROFILMED
EXACTLY AS RECEIVED

AVIS

La qualité de cette microfiche dépend grandement de la qualité de la thèse soumise au microfilmage. Nous avons tout fait pour assurer une qualité supérieure de reproduction.

S'il manque des pages, veuillez communiquer avec l'université qui a conféré le grade.

La qualité d'impression de certaines pages peut laisser à désirer, surtout si les pages originales ont été dactylographiées à l'aide d'un ruban usé ou si l'université nous a fait parvenir une photocopie de qualité inférieure.

Les documents qui font déjà l'objet d'un droit d'auteur (articles de revue, examens publiés, etc.) ne sont pas microfilmés.

La reproduction, même partielle, de ce microfilm est soumise à la Loi canadienne sur le droit d'auteur, SRC 1970, c. C-30.

LA THÈSE A ÉTÉ
MICROFILMÉE TELLE QUE
NOUS L'AVONS REÇUE

THE UNIVERSITY OF ALBERTA

A SCHLIEREN STUDY OF FLAME INITIATION

by

RICHARD F. HALEY

A THESIS

SUBMITTED TO THE FACULTY OF GRADUATE STUDIES AND RESEARCH
IN PARTIAL FULFILMENT OF THE REQUIREMENTS FOR THE DEGREE
OF MASTER OF SCIENCE

DEPARTMENT OF ELECTRICAL ENGINEERING

EDMONTON, ALBERTA

SPRING 1986

SEP 77

Permission has been granted to the National Library of Canada to microfilm this thesis and to lend or sell copies of the film.

The author (copyright owner) has reserved other publication rights, and neither the thesis nor extensive extracts from it may be printed or otherwise reproduced without his/her written permission.

L'autorisation a été accordée à la Bibliothèque nationale du Canada de microfilmer cette thèse et de prêter ou de vendre des exemplaires du film.

L'auteur (titulaire du droit d'auteur) se réserve les autres droits de publication; ni la thèse ni de longs extraits de celle-ci ne doivent être imprimés ou autrement reproduits sans son autorisation écrite.

ISBN 0-315-30224-0

THE UNIVERSITY OF ALBERTA

RELEASE FORM

NAME OF AUTHOR RICHARD F. HALEY
TITLE OF THESIS A SCHLIEREN STUDY OF FLAME INITIATION
DEGREE FOR WHICH THESIS WAS PRESENTED MASTER OF SCIENCE
YEAR THIS DEGREE GRANTED SPRING 1986

Permission is hereby granted to THE UNIVERSITY OF ALBERTA LIBRARY to reproduce single copies of this thesis and to lend or sell such copies for private, scholarly or scientific research purposes only.

The author reserves other publication rights, and neither the thesis nor extensive extracts from it may be printed or otherwise reproduced without the author's written permission.

(SIGNED) *R. Haley*

PERMANENT ADDRESS:

#708-11135-83ave
Edmonton Alta
T6G 2C6

DATED *Jan 31* 19 *86*

THE UNIVERSITY OF ALBERTA
FACULTY OF GRADUATE STUDIES AND RESEARCH

The undersigned certify that they have read, and recommend to the Faculty of Graduate Studies and Research, for acceptance, a thesis entitled A SCHLIEREN STUDY OF FLAME INITIATION submitted by RICHARD F. HALEY in partial fulfilment of the requirements for the degree of MASTER OF SCIENCE in ELECTRICAL ENGINEERING.

.....
Supervisor

.....
.....
.....

Date.....Jan 31, 1956.....

Abstract

A high speed schlieren camera system is described which allows the recording of flame kernel development at speeds of up to twelve thousand frames per second. Each frame was illuminated for only one hundred nanoseconds to provide sharp images, including those of the shock waves produced by the electric discharge.

Photographs of the flame kernels in three mixtures of methane and air show a definite increase in flame speed with ignition by short duration sparks. Flame kernels ignited by short duration sparks were more turbulent and expanded faster than flame kernels ignited by longer duration sparks of the same energy.

Acknowledgements

I would like to thank Peter Smy for the opportunity to write this thesis, Doug Way-Nee for his help in the construction of several key components for the experiments and Doug Dale for his concise explanations concerning combustion. Many useful, one-sided conversations with Steven Au and Ewen Nelson corrected problems faster than would otherwise have been possible. The production of this thesis was made easier by my mother, Eva, possibly the fastest and most accurate proof-reader in Edmonton.

Table of Contents

Chapter	Page
1. Introduction	1
2. Schlieren Photography	5
2.1 Light Source	10
2.2 Parallel Beam Section	12
2.3 Camera Section	14
2.4 Test Section	16
3. High Speed Camera	17
3.1 Light Source	21
3.2 Laser Diode Theory	22
3.3 Laser Diode Power Supply	27
4. Experimental Method	30
4.1 Spark Power Supplies	32
4.2 Data Collection	38
5. Spark Thermal Efficiency and Interferometry	46
5.1 Thermal Efficiency	46
5.2 Interferometry	52
6. Summary	57
References	62

List of Tables

Table	Page
1 SPARK DATA	33
2 FLAME TRAVEL IN 5 MS COMPARED TO THE ONE JOULE, 50 μ S SPARK	44
3 VOLUME BURNING IN 5 MS COMPARED TO THE ONE JOULE 50 μ S SPARK	44
4 VARIATION OF FLAME TRAVEL WITH MIXTURE RATIO	45
5 SPARK EFFICIENCIES	47

List of Figures

Figure	Page
1 Parallel Beam Schlieren	6
2 Schlieren Using a Knife Edge	6
3 Schlieren Using an Iris	6
4 Experimental Layout	9
5 Pulsed Laser Diode Power Supply	28
6 Discharge Power Supply; 50 μ s, 1 Joule	34
7 Fast Discharge Power Supply	37
8 Effect of Spark Source on Flame Front Travel $\lambda = 1.0$	40
9 Effect of Spark Source on Flame Front Travel $\lambda = 1.2$	41
10 Effect of Spark Source on Flame Front Travel $\lambda = 1.5$	42
11 Mach-Zehnder Interferometer	53
12 Test Cell Layout for Interferometry	53

List of Plates

Plate	Page
1 Typical SP 2000 Display	18
2 Current Waveform for the 50 μ s Spark	35
3 Typical Current Waveform for the Fast Sparks	35
4 Typical Series of Flame Growth Photographs	39
5 Typical Efficiency Test Output	47
6 Oscilloscope Output From Interferometer	55
7 Oscilloscope Output From Interferometer Showing Little Pressure Rise During the First Ten Milliseconds	55
8 Fast Discharge Flame Kernel; t=1 ms.	58
9 Slow Discharge Flame Kernel; t=1 ms.	58

1. Introduction

This work describes a high speed schlieren camera system with a pulsed laser diode light source and its use in the study of the ignition of combustible mixtures. The effect of spark duration in the ignition of methane in air was studied as an example of the use of this system.

Ordinary pictures of the visible flame, while showing the flame front, provide little information about the flame structure behind the front. Turbulence, in particular, shows up very clearly in schlieren photographs (Keck, 1982).

Air pollution and the increasing cost of gasoline both exert pressure on society to develop more efficient and cleaner burning engines for automobiles. Lean burn engines have the potential for increasing the efficiency of the automobile. At the same time pollution generated by the engines may be reduced (McGeer and Durbin, 1982). For the past decade research into lean burn internal combustion engines and alternate fuels has increased. In Canada, with its relative abundance of natural gas, automobiles fueled by methane are a logical choice for future transportation. Unfortunately, methane exhibits a lower flame speed than gasoline and the flame speed of

methane is reduced with increasing pressure. Due to the increased ignition delay advanced ignition timing is required by internal combustion engines fueled by methane. The increased burning time due to a longer ignition delay and slower flame speed result in a loss of power and efficiency, reducing the attractiveness of this fuel (Gettel and Tsai, 1983). In addition, operating an internal combustion engine with any lean fuel-air mixture results in increased burning time, requiring advanced spark timing, again causing a loss of power and efficiency. If combustion duration for these two cases could be reduced substantial savings in gasoline would result.

Maly and Vogel (1979) found that if the spark source can add more energy to the flame kernel before the flame front develops, the kernel will be larger and the initial flame speed will be increased. It has been demonstrated that very short duration (<100 ns) spark sources show a greatly increased efficiency for changing the electrical energy from the source to thermal energy in the gas (Maly, 1980). The more rapidly the spark energy is deposited in the gas, the higher is the resulting initial flame speed. A standard automobile spark has an energy of about thirty

millijoules and a typical duration of one millisecond (Oberts 1973).

For the purposes of these experiments short duration (1 microsecond) sparks of three different energies were compared to a one joule, fifty microsecond spark, with the latter spark being the standard. Four sparks were chosen for this investigation. To make any differences easier to measure a large (one joule) stored energy was used. For simplicity, the fifty microsecond discharge will sometimes be referred to as the 'slow' spark and the submicrosecond discharges are sometimes called the 'fast' sparks.

Schlieren photography, an elegant method for flame position measurements, is presented in Chapter Two. The Kodak Spin Physics SP 2000 Motion Analysis System (SP 2000) provides sequential photographs of each flame trial and is described in Chapter Three. The laser diode light source used to illuminate the schlieren system to photograph the flame is also presented in Chapter Three. Chapter Four describes the experimental set up. The characteristics of the sparks and the power supplies which create them are also found in Chapter Four. The results of the flame travel measurements using four different sparks in three different fuel-air mixtures is discussed as well.

The investigations of spark efficiencies and pressure changes in the test cell are presented in Chapter Five. It was found that the thermal efficiency of the two one joule sparks were different. Chapter Five describes the experiment and equipment used to measure the spark efficiencies. The efficiency test cell was used to find the energy of the fast discharge which put the same amount of thermal energy into the gas as the one joule, fifty microsecond spark.

The mixture ratio is denoted λ where

$$\lambda = \frac{\text{stoichiometric mixture volume ratio}}{\text{actual mixture volume ratio}}$$

The stoichiometric ratio for methane in air is 9.5 percent by volume (Lewis and von Elbe, 1961). Three mixtures of methane and air were investigated. These were $\lambda = 1.0$, $\lambda = 1.2$ and $\lambda = 1.5$.

2. Schlieren Photography

Schlieren is defined as: regions of varying refraction in a transparent medium often caused by pressure or temperature differences and detectable especially by photographing the passage of a beam of light (Webster's, 1973). There are many variations of schlieren photography depending on the light source, the test section and the lenses available. These experiments used the single pass, parallel beam, z-geometry version as shown in Figure 1.

When a parallel beam is focussed to a point and a knife edge intercepts the focus, no light is transmitted to the camera. However, if the parallel light is disturbed by regions of different refractive index some of the light will not be focussed at the knife edge. These perturbed rays will either be blocked by the knife edge or pass over it to the camera [Fig.2]. Refractive index in gases varies with temperature. Parallel beam schlieren photography sends a collimated beam of light through the test section containing, in this case, the early stages of a methane-air flame. The flame is hot compared to the surrounding gas so its refractive index is lower and the light which passes obliquely through the edge of the flame

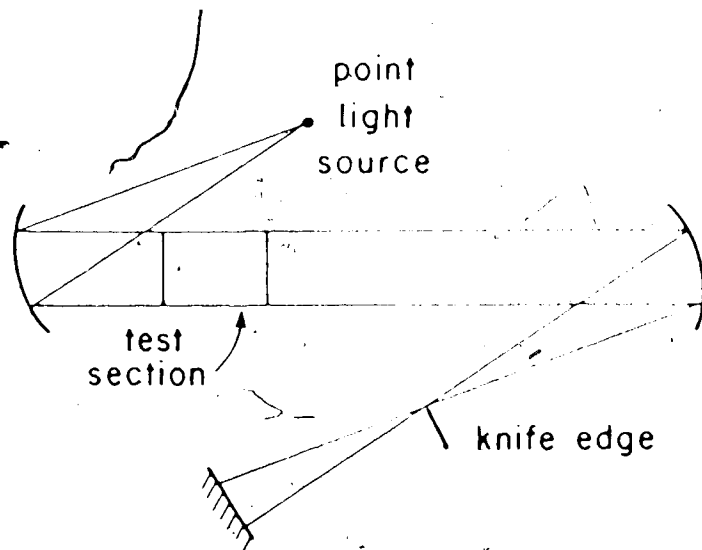


Figure 1 Parallel Beam Schlieren

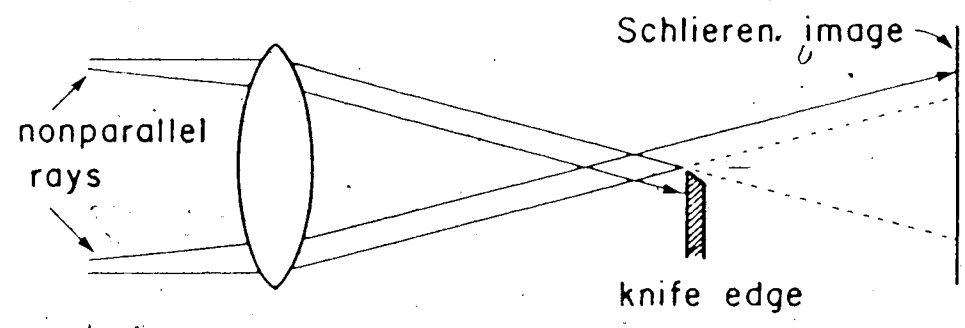


Figure 2 Schlieren Using a Knife Edge.

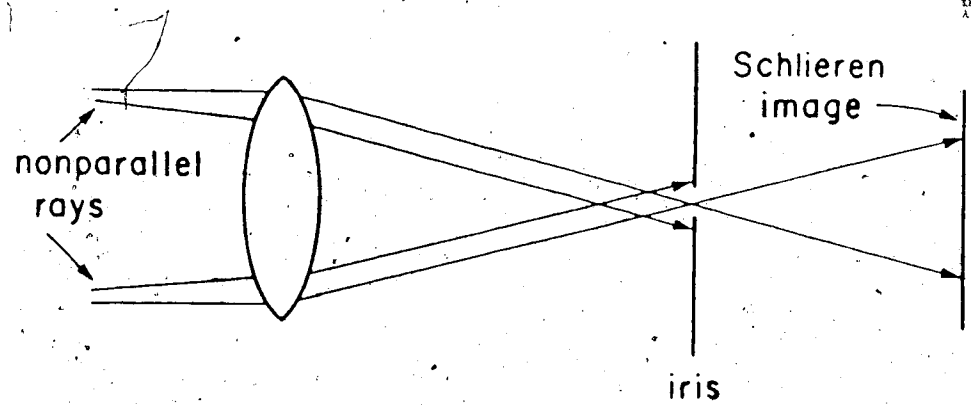


Figure 3 Schlieren Using an Iris

is deflected toward the cold gas with its higher index of refraction. Light which enters and exits the flame through a perpendicular face of the flame front is relatively undisturbed. Thus the light which has passed through the leading edge of the flame front is deflected past the knife edge and is recorded on the photograph (Weinberg, 1963).

Many light sources were tried here but all were focussed and passed through an iris to form a point source with the desired beam divergence. If a point source is placed at the focus of a concave spherical mirror the result is a parallel light beam. This parallel light passes through the test section and is collected by another concave spherical mirror. Since the light collected by the second mirror is parallel, it is focussed to a point given by the focal length of the mirror. At this point a knife edge is placed to just intercept the spot of light at the focus. In this case some of the deflected rays reach the camera and some of the light is blocked by the knife edge. The amount of light blocked by the knife edge at the focus determines the brightness of the background. Intercepting more of the light makes the background darker and increases the contrast of the system

since the deflected light shows up more clearly on a dark background. If the knife edge blocks more than the focal point the system is less sensitive to small changes in refractive index since more of the deflected light is stopped.

Flames generally have a large difference in refractive index from air or the unburnt fuel-air mixture. Using a reduced sensitivity causes the photographs to show a greater range of deflections. For conditions where the camera requires more light the knife edge can be replaced by an iris. The light which was previously blocked by the body of the knife edge can now reach the camera. The background light is unimpeded and the deflected light is blocked by the iris. This method is less sensitive, but in flame studies the loss in sensitivity is more than offset by the gain in light intensity [Fig.3]. The sensitivity of the system also depends on the focal length of the collecting mirror. A longer path from the test section to the mirror increases the sensitivity since a deflected ray will be farther from its expected position.

The basis for these experiments is a schlieren camera system which can photograph results on Polaroid film, 35mm film, or on magnetic video tape [Fig.4]. The schlieren

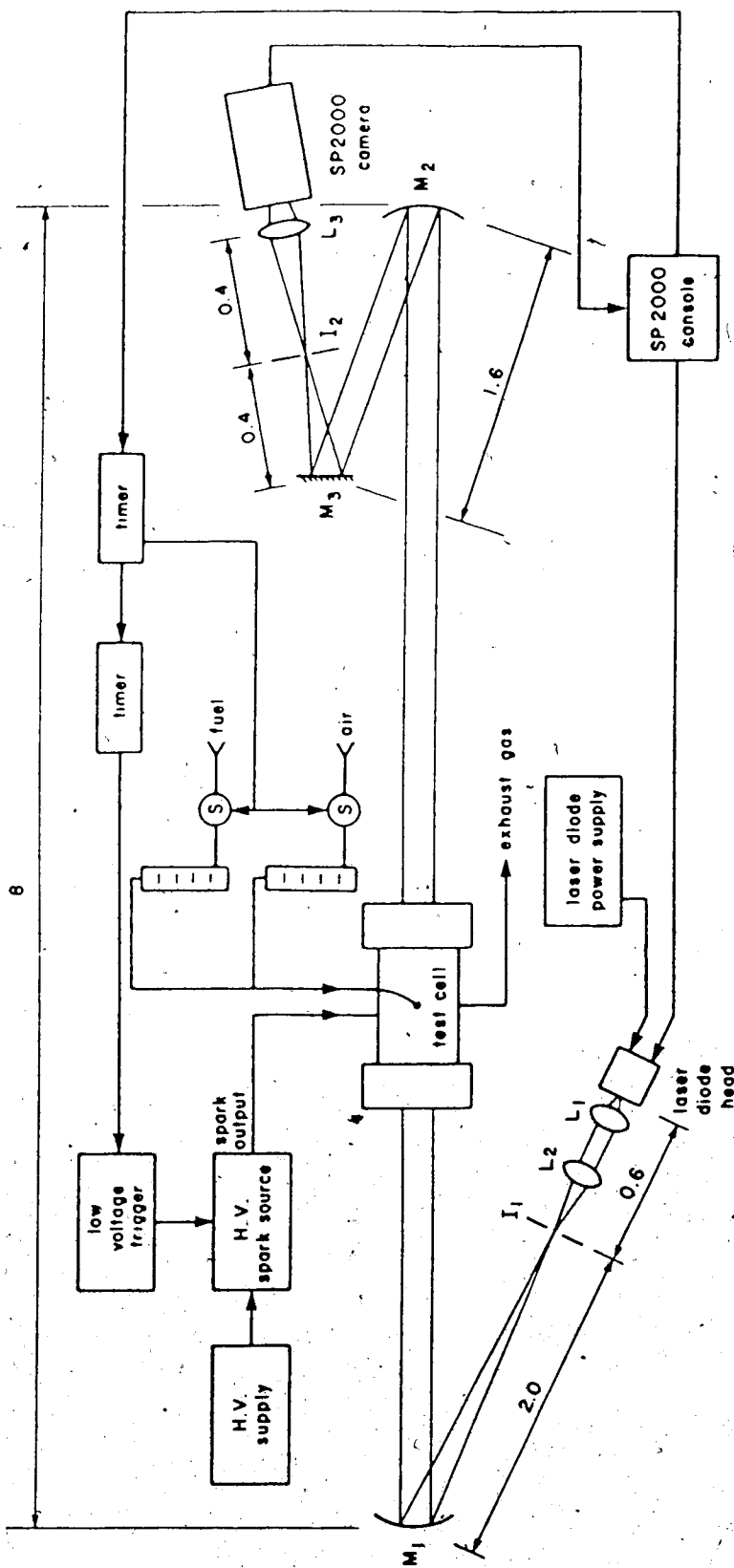


Figure 4 Experimental Layout

system used in this study utilized fifteen centimeter diameter front surface concave spherical mirrors with a two hundred centimeter focal length, so the parallel beam should be four meters long. However, due to problems with electrical interference in the SP 2000 camera, the distance between the two mirrors was increased to eight meters.

2.1 Light Source

The light sources which were tested and rejected included a tungsten halogen light bulb, an electric discharge from a plasma plug (which can be augmented by firing into Argon), or a ten milliwatt Helium-Neon laser. Final experiments used a pulsed thirty watt laser diode (RCA SG 3001) emitting at 904 nm.

Several lenses are required to form the laser beam into a point source with the desired divergence. Each lens adds aberrations to the laser light, and photographs illuminated by a Helium-Neon laser suffered from a great deal of interference and laser speckle. Interference and laser speckle are related to the coherence of the light source. Coherence length is a function of the bandwidth of the light source.

The laser diode has a relatively broad bandwidth compared to the Helium-Neon laser so the coherence length is much shorter. If two light waves travel paths which differ in length by more than the coherence length then interference between the two waves will be sharply reduced.

If the laser light passes through or reflects off a surface whose roughness is less than the coherence length but greater than the wavelength of the light, laser speckle occurs. It is due to the surface shifting the phase of the light without destroying the temporal coherence. When the light is imaged on a camera the wavefronts arrive out of phase, but are still coherent. This gives rise to interference patterns of the same scale as the diffraction limit for the light in use.

Coherence length (l_c) is a function of the wavelength (λ) of light and the spectral bandwidth ($\Delta\lambda$) (Dainty, 1984).

$$l_c = \frac{\lambda^2}{\Delta\lambda}$$

For the RCA SG 3001 laser diode $\lambda = 904 \text{ nm}$ and $\Delta\lambda = 3.5 \text{ nm}$ at the half power points. Therefore, the coherence length

is expected to be approximately 0.2 millimeters. In the schlieren system the laser diode light is reflected from an inclined spherical mirror at an angle of about 140 mrad. This causes an optical path difference of more than six millimeters before the light has even reached the test section. Since the path length difference (6 mm) is greater than the coherence length (0.2 mm) significant interference was not a problem when using the laser diode as a light source (Clarke et al, 1985).

Other reasons for using the laser diode are that it is simple to operate, low cost and generates no appreciable amount of heat. It is effectively a point source and can be pulsed to 'freeze' the motion for the camera.

2.2 Parallel Beam Section

The parallel beam was normally eight centimeters in diameter with a divergence of less than 0.3 mrad. The advantages of the parallel beam system over the diverging beam is that the source appears to be at infinity and the collecting mirror has the same dimensions as the test space. Having the source at infinity improves the sensitivity of the schlieren, but requires more optical

components. In the diverging beam case the collecting mirror must be larger than the test space which requires more expensive optical components.

The laser diode light was collected by two short focus lenses which form a variable focal length system [Fig. 4]. These lenses collect the laser light and focus it at the focal point of a concave spherical mirror. The light is reflected from the mirror as a parallel beam. Since the parallel beam should not be blocked by the source lenses the light must be off axis to the mirror. Because the mirror was spherical the off axis requirement caused astigmatism and coma in the camera optics. The effect of coma was eliminated, at least for first order effects, by using two identical mirrors at the ends of the parallel beam and by reflecting the beam once to the right and once to the left [Fig. 1]. Astigmatism was found to be a severe problem when a one centimeter focal length lens was used for collecting the laser diode light. This astigmatism was created by the laser diode and the mirrors only aggravated the situation. Consequently a five centimeter collecting lens was used in front of the laser diode in the final design.

2.3 Camera Section

The camera section consisted of the collecting schlieren mirror, a marking aperture, a magnifying lens and a camera. For setups with severe astigmatism the 'normal' schlieren knife blade marking aperture must be used with its edge parallel to one of the astigmatic planes. Otherwise the blade will block different amounts of light in the two planes and poor schlieren sensitivity will result. The circular aperture allows more light to reach the camera at the expense of sensitivity but the astigmatism must be reduced to produce useful results. Here the problem was sufficiently reduced by removing the laser diode induced astigmatism and leaving the spherical mirror contributions uncorrected.

The knife edge marking aperture showed a refractive index gradient perpendicular to the knife edge as a black edge on one side of the photograph and as a white edge on the other side. A refractive index gradient parallel to the knife edge does not show at all in the photographs. However, the flame fronts studied here were basically spherical and a circular marking aperture showed all the gradients, regardless of direction, as a black edge. Thus the circular aperture allowed more light to reach the

camera and also removed the polarity of the refractive index gradient from the photographs.

The camera section has been used with Polaroid film and 35 mm negatives on a box camera for still photos. The Polaroid provides quick results for alignment and focussing while the 35 mm film gives sharper definition, more tones of gray, and ease of reproduction and enlargement in the darkroom. The SP 2000 gives continuous video capability so that changes may be seen immediately. Only the SP 2000 can image the 904 nm light from the laser diode without added complications. The major drawback of the SP 2000 is the image quality which is worse than that of a Polaroid photograph.

There are four major advantages to the SP 2000 approach: fast results, tape storage, sequential photos and adjustable playback. Fast results means that the data can be checked immediately, typically in seconds. Tape storage allows the accumulation of vast records that would soon become voluminous and confused if stored on photographs. The SP 2000 information may be played back and photographed at a later date if required. Sequential photos of the same event are useful in removing the scatter in results. Previously, single photographs taken

at different times and of different events were put in sequence. Because of random effects no two shots were the same. The SP 2000 is described in Chapter Three.

2.4 Test Section

A cylindrical steel test cell ten centimeters long and eight centimeters in diameter with glass windows at each end was placed in the test section. It was then filled with a methane-air mixture and ignited. The motion of the flame front was plotted using the schlieren images, and various mixtures and spark sources were compared. The test section in a parallel beam schlieren is normally located between one and two times the focal distance from the collecting mirror. A distance greater than one focal distance is required to form a real image of the test space in the camera. For these experiments the test space was located three focal lengths from the camera to increase the separation of the camera and power supplies due to problems with noise generated by electrical interference. Information was lost when the electromagnetic shielding of the spark source or the camera head was insufficient.

3. High Speed Camera

The camera used to record the schlieren images was a Kodak Spin Physics SP 2000 Series II Motion Analysis System (SP 2000). This system consists of a photocapacitive array with its associated electronics in a small housing connected by a cable to the main control unit. The main unit contains a high speed digital to analog converter and an analog tape recorder capable of recording two thousand frames of video data per second. Each frame of data is made up of one hundred ninety-two lines each with a resolution of two hundred and thirty-eight pixels per line. This unit puts out a standard NTSC video signal so that the output can be viewed on a standard monitor. Betamax, VHS, or other video tape recorders can be used to store, edit or display the information recorded by the camera. A typical SP 2000 display is shown in Plate 1.

The keyboard on the main unit allows the user to record, play back and alter the recording speed and format. Playback can occur at one, two, three, four or sixty frames per second. Each recording tape is three hundred meters long and lasts from fifty seconds to thirty minutes depending on the recording speed.



Plate 1 Typical SP 2000 Display

The photocapacitive array of the camera is scanned once per frame so the exposure time is equal to the inverse of the recording speed. No independent shuttering is provided. By increasing the framing rate the exposure time is reduced, which freezes the images of faster moving events. The lowest possible framing rate is desirable to reduce the amount of tape used and to increase the depth of field. Since a slower scan rate makes the pictures appear brighter due to the longer exposure time a smaller aperture may be used. As the size of the aperture is reduced, the depth of field is increased.

At a given framing rate it is also possible to increase the camera speed by splitting the screen into two, three or six strips horizontally. This means that the area viewed becomes smaller, but for some events that occur horizontally to the camera this reduction is not important. At two thousand frames per second the tape recorder has reached its maximum speed. However, by splitting the screen, the speed of the camera can be increased to four, six or twelve thousand pictures per second without requiring a faster tape recorder. The exposure time with a split screen is the inverse of the product of the frame rate and the frame format.

As shown in Plate 1, the SP 2000 has an information border surrounding the camera image when the data is displayed on a monitor. Data displayed on the SP 2000 monitor can be measured with an 'on screen' reticle. The data border displays the x and y coordinates when the reticle is activated. Integers from one to one hundred ninety-two represent the y coordinates and from one to two hundred and thirty-eight for the x coordinates. If an object on the monitor has a known dimension the reticle can measure it to calibrate the scale of the data. From then on quick calculations yield the size and velocity of subsequent events. Time, date, frame number, framing rate, elapsed time, tape counter, motion of the tape and the source of the image are displayed in the information border.

Strong electromagnetic noise generated by the experiment required that the camera head be shielded by a conducting cloth woven of cotton with twenty percent nickel. The nickel cloth was required to cover the entire camera and was connected to the cable shield covering the long camera cable which connects the head to the main control unit.

3.1 Light Source

Because the exposure time is inversely proportional to the framing rate and the camera is roughly equivalent to one hundred ASA film, the amount of light required for high speed photography becomes excessive. For example, at five hundred frames per second three six hundred watt tungsten halogen light bulbs are required to illuminate an area of one square foot. For this reason backlighting photography is desirable for framing speeds over five hundred per second.

A weak shock wave in air travels at roughly three hundred meters per second. For a camera to stop the image of a shock wave to within one-tenth of a millimeter requires an exposure time of about three hundred nanoseconds. For ten consecutive frames showing the travel of a shock wave across a thirty centimeter field of view a framing speed of twelve thousand per second is required. Present strobe light systems are able to produce the necessary pulse duration, but none are bright enough when operating at twelve thousand hertz. For this reason a pulsed laser diode was chosen as the light source.

Control circuitry was designed to fire the laser diode once per camera frame so that no adjustments to the

illumination were required even though the framing rate changed by two orders of magnitude, from sixty to twelve thousand hertz. This allowed the equipment to be set up, focussed and aligned at a low framing rate to reduce the thermal stress on the laser diode. Once the equipment was ready to record data, only the camera framing rate needed to be changed. All other variables remained constant without affecting the quality of the photographs produced.

When this camera system was used with a continuous light source the photographs showed a great deal of blurring even at the highest framing rates. Continuous light sources required adjustment in brightness whenever the framing rate was changed. Controlling the brightness of a Helium-Neon laser was accomplished using an adjustable iris.

3.2 Laser Diode Theory

The type of laser diode best suited for use as a light source in backlighted flash photography was the gallium-arsenide single heterojunction laser diode. The discussions in Section 3.1 show that the photographic light source should be able to produce pulses less than three hundred nanoseconds long, at a rate of twelve

thousand hertz. Gallium-arsenide single heterojunction laser diodes provide high power at a low duty cycle. Double heterojunction laser diodes presently do not provide enough power when operated at submicrosecond pulse widths.

The RCA SG 3001 laser diode used here typically had an emitting region of $228 \times 2 \mu\text{m}$. The active region in a GaAs laser is in the p-doped side of the p-n junction. Since the lasing region must be contained on all sides a p-GaAlAs layer is grown on top of the p-GaAs. This forms the single heterojunction. The GaAlAs layer has a higher bandgap than the p-GaAs to help confine the carriers in the active region. The refractive index of p-GaAs is higher than that of the outer layers so the laser radiation is confined to the active layer by internal reflections at the top and bottom faces. The sides of the active region are sawn to produce nonreflective faces so that cross modes are not amplified. To form a partially reflecting Fabry-Pérot cavity, the front and back surfaces are cleaved along parallel planes and a mirror installed on the rear face.

When the current density across the p-n junction exceeds the threshold of about eight thousand amperes per

square centimeter a population inversion is created which leads to stimulated emissions. The Fabry-Pérot construction of the cavity amplifies the stimulated emissions and the laser light is emitted from the front facet. Since the laser is based on band transitions, the spectral width of the output is wider than that of lasers which depend on discrete transitions such as the Helium-Neon gas laser (Fabian, 1981). Because the cavity dimensions are so close to the wavelength of the light emitted, strong diffraction effects produce a very divergent output beam.

Experiments began using an RCA SG 2006 laser diode emitting at 904 nm with a pulse duration of sixty nanoseconds and a maximum power of seven watts. Since laser diodes produce very divergent beams they naturally make a very good point source. The seven watt laser diode was found to be inadequate for the size of the system and was replaced by a thirty watt stacked laser diode array consisting of three ten watt laser diodes in series. Because of the small size of the laser diodes, the three stacked laser chips still appeared as a point source to the system. The thirty watt SG 3001 provided a pulse width of eighty nanoseconds also at 904 nm. The SP 2000 is

sensitive to radiation with wavelengths from five hundred to one thousand nanometers, so the laser diode light at 904 nm is visible to the camera, although it is invisible to the human eye. The experiment was aligned using an infrared viewer until the light was visible on the monitor. Then, using small adjustments to keep the light visible on the monitor, the system was fine-tuned by trial and error to achieve a uniform background illumination.

One major drawback to the laser diode was beam quality. Because the emitting facet is 228 by 2 μm the beam has an elliptical cross section. The divergence in the plane parallel to the junction is typically half the divergence in the plane perpendicular to the junction. The RCA SG 3001 is a gain-guided laser diode, which means the laser light is confined by the electric current profile in the plane parallel to the junction and by internal reflections in the plane perpendicular to the junction. In the plane parallel to the junction the beam appears to radiate from a point twenty to fifty micrometers behind the emitting facet, while perpendicular to the junction the light appear to originate from the facet itself. When the light is collected and refocussed, the light in the two planes will focus at different locations. This

astigmatism becomes worse when the light is collected by a very short focal length lens and also when a low f-number lens is used. Unfortunately, a short focus lens with a low f-number must be used to collect as much light as possible because of the strongly divergent beam. Anamorphic prism pairs may be used to equalize the divergence in the two planes to yield a circular beam profile, and a weak cylindrical lens can reduce the astigmatism (Melles-Griot, 1985). By reducing the astigmatism and the differences in divergence the beam may be focussed to a smaller spot and this will increase the schlieren sensitivity. The laser diode is sold in a stud-mount package with a flat glass window about one-half millimeter thick. Because the window reduces the output of the laser beam and introduces aberrations, the window was removed for some experiments. Removing the window did increase the laser brightness, but the ruggedness of the source was severely compromised. A five centimeter diameter aspheric lens with a focal length of six centimeters was mounted about six centimeters from the laser diode. The purpose of this lens was to collect the laser light into a nearly parallel beam.

A five centimeter diameter, fifteen centimeter focal length lens collected the parallel light and brought it to

a focus. The two lenses form a variable focal length system to allow a variable beam divergence which depends on the size of the parallel beam desired. A small beam divergence will illuminate a smaller area, but the light intensity will be increased. Alignment of the system is critical. The laser diode and the first collecting lens must be aligned within tens of micrometers relative to each other. The mirrors must be aligned to within 1.7 mrad.

3.3 Laser Diode Power Supply

The laser diode system was of original design and underwent several modifications [Fig.5]. The final system consisted of a laser head connected by a cable to the power supply and by a coaxial cable to the SP 2000 strobe output. The strobe output triggered the laser diode in synchrony with the camera frame through a pulse transformer in the laser head. The laser diode head measured five centimeters high, eight centimeters long and three centimeters thick, and was mounted on a three axis stage on an optical bench for alignment. The power supply charged a large ($15\mu\text{F}$, 1000V) oil-filled capacitor to a variable DC voltage (0 to 600 V) as selected by the front

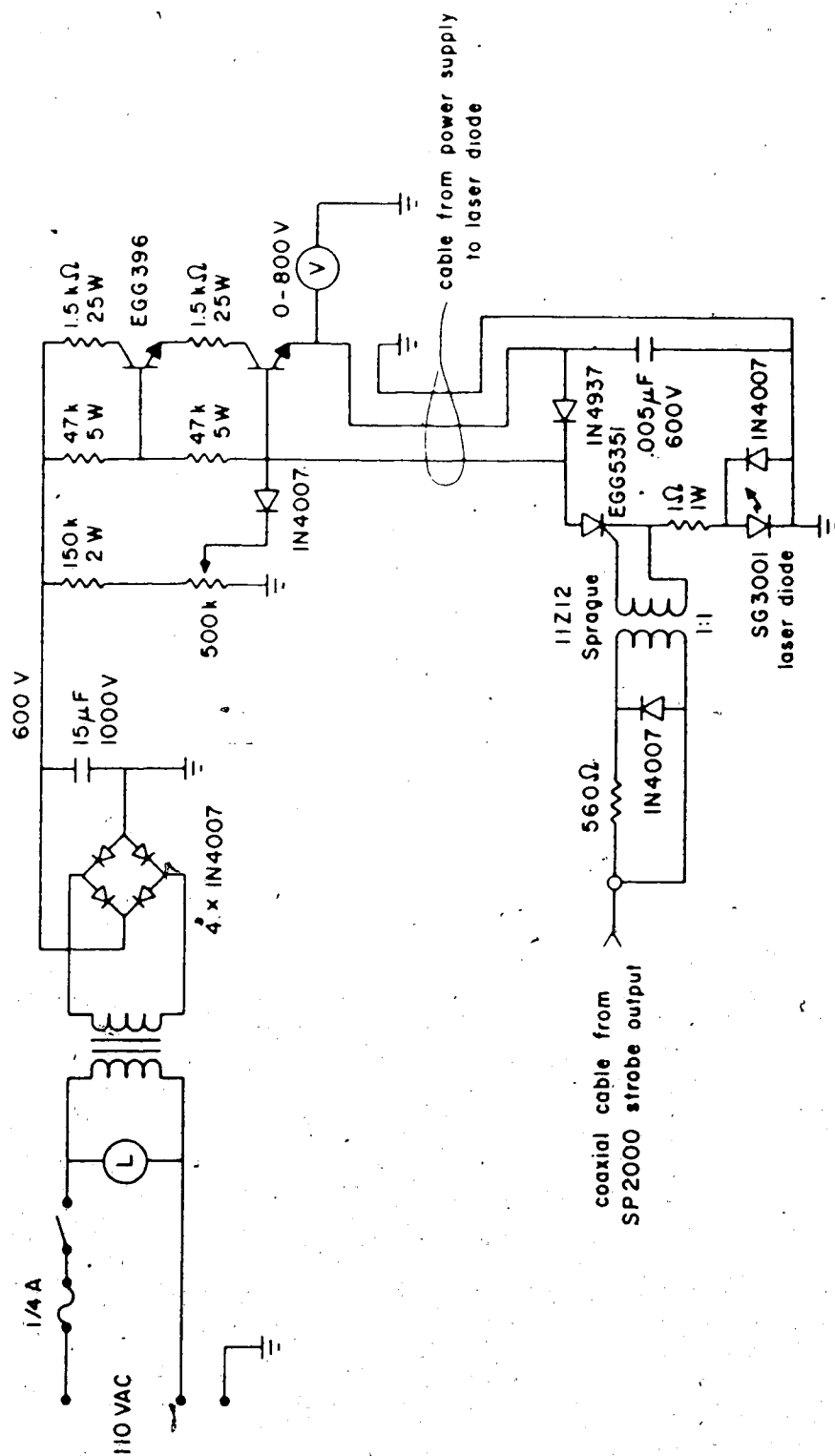


Figure 5. Pulsed Laser Diode Light Source

panel controls. A simple transistor circuit allowed the DC voltage to charge a small capacitor in the laser head only after the silicon-controlled rectifier had shut off from the previous pulse. The fast recovery silicon-controlled rectifier in the laser head discharged the capacitor through the laser diode and recovered within eight microseconds. This allowed charging to be complete within the eighty microseconds available when the camera is operating at twelve thousand hertz. By varying the small capacitor in the laser head the pulse width could be altered, and by changing the charging voltage the brightness of the diode could be controlled. For most applications the small capacitor was five nanofarads and the charging voltage was six hundred volts (Fabian, 1981).

4. Experimental Method

The purpose of these experiments was to study the effects of different sparks on the ignition of a methane-air mixture. The SP-2000 schlieren system viewed a glass windowed test cell to yield measurements of flame travel [Fig.4]. Because the flame pushes the unburnt mixture in front of it, the system measures the speed of travel of the flame, not the true burning velocity of the flame relative to the unburned mixture. The test cell enclosed a cylinder ten centimeters long and eight centimeters in diameter for a volume of five hundred cubic centimeters. Methane was mixed with air and allowed to flow through the test cell until ten seconds had elapsed. This allowed five volumes of a known mixture to pass through the test cell and was enough to clear out the gases left by the previous test. Two outlets with sintered filters for flame arrestors allowed the pressure to escape as the flame filled the test cell.

Since measurements were complete before the burning, volume exceeded ten percent of the test cell volume, no appreciable pressure rise occurred to alter the flame speed from its free-air value. Later experiments discussed in Chapter Five confirm this fact. A J-shaped spark gap

fashioned from one millimeter diameter steel wire reached into the center of the test cell to reduce the effects of the cold walls on the flame. Results presented here were obtained using a spark gap of two millimeters.

Measurements were taken only in the horizontal direction to the right of the spark source as seen in Plate 4.

Simple timing circuits were constructed to provide the same initial conditions for each trial. The first circuit operated solenoids to allow the fuel-air mixture to flow for ten seconds through Fisher-Porter rotameters (Model No. 10A3135N) to measure the mixture ratio. Since the rotameters were calibrated for air, the meter on the methane source was used to hold the flow constant, and the flow was measured separately by the displacement of water. To measure the rate of flow of the methane a graduated flask filled with water was inverted in a larger tank of water and the methane outlet was placed inside the flask. Measurements of the time required for the methane to displace the water allowed the calculation of the methane flow rate. The flow through the test cell was stopped ten seconds before the mixture was ignited.

When a smoke plume was introduced into the test cell the movement of the smoke indicated very small gas

velocities after ten seconds. This showed that the turbulence had subsided and the initial mixture could be considered quiescent.

Timing signals from the SP 2000 strobe interface allowed the spark to fire only when it was synchronised to the camera frame. Photographs showing the shock wave from the spark often show a timing repeatability within twenty microseconds. To eliminate shot-to-shot variations in flame position three to five trials were averaged for each spark and mixture combination. In lean mixtures the data after ten milliseconds was repeatable to within twelve percent, and in a stoichiometric mixture the data varied by only four percent.

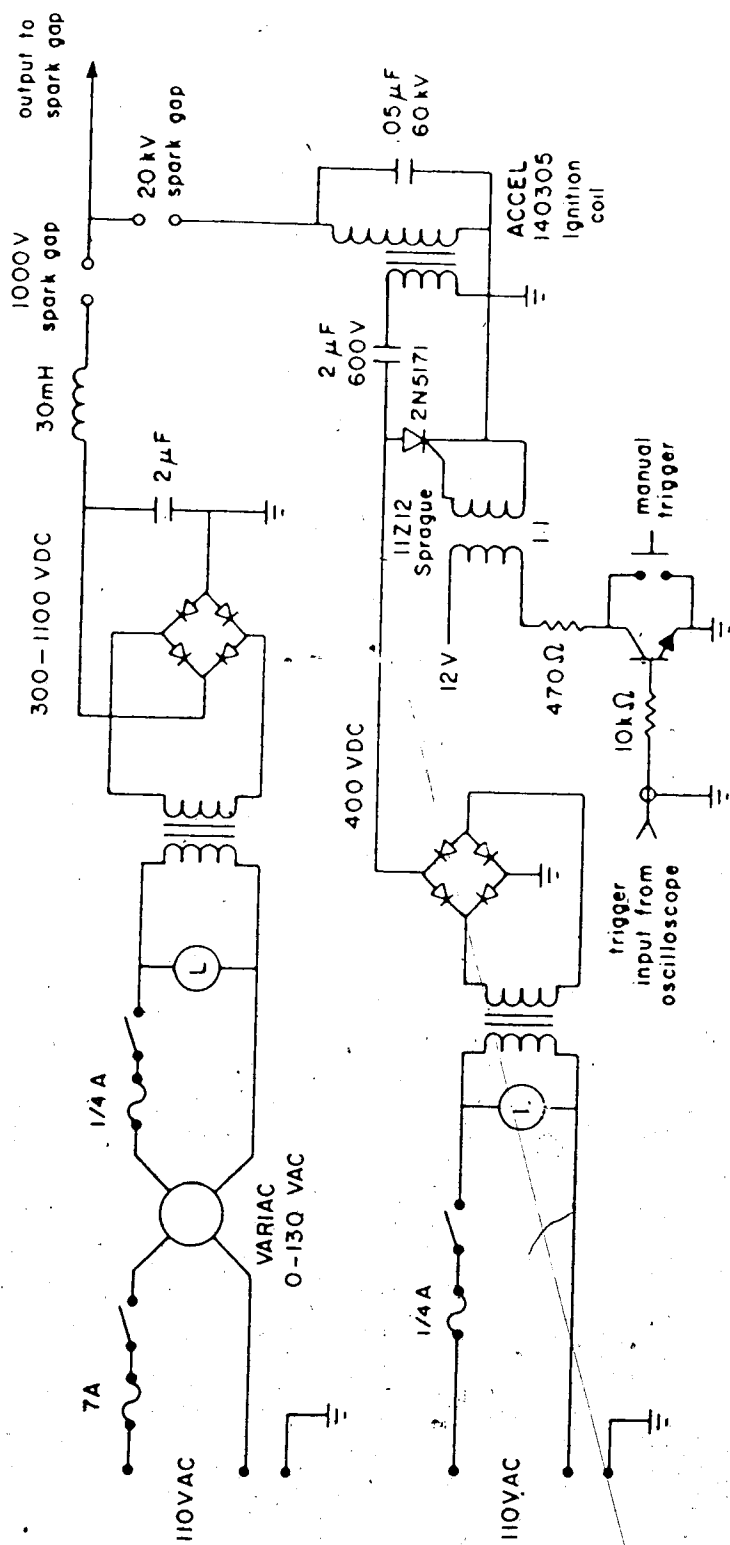
4.1 Spark Power Supplies

Four sparks with different characteristics were used in these experiments [Table 1]. A spark with a duration of fifty microseconds was generated by an overvolted capacitive discharge power supply [Fig.6][Plate 2]. A two microfarad capacitor was charged to one kilovolt to store one joule of energy. Another circuit generated a high voltage low energy spark to breach the series gap and to release the stored energy of the large capacitor through

TABLE 1

SPARK DATA

<u>Energy</u> <u>(Joules)</u>	<u>Duration</u> <u>(Seconds)</u>	<u>Voltage</u> <u>(Kilovolts)</u>	<u>Capacitance</u> <u>(Nanofarads)</u>
1.0	50 X 10 ⁻⁶	1.0	2000
1.0	800 X 10 ⁻⁶	27.0	2.70
0.6	700 X 10 ⁻⁶	21.0	2.70
0.1	500 X 10 ⁻⁶	20.0	0.57



* all diodes IN4007

Figure 6 Discharge Power Supply - 50 μ s, 1 Joule

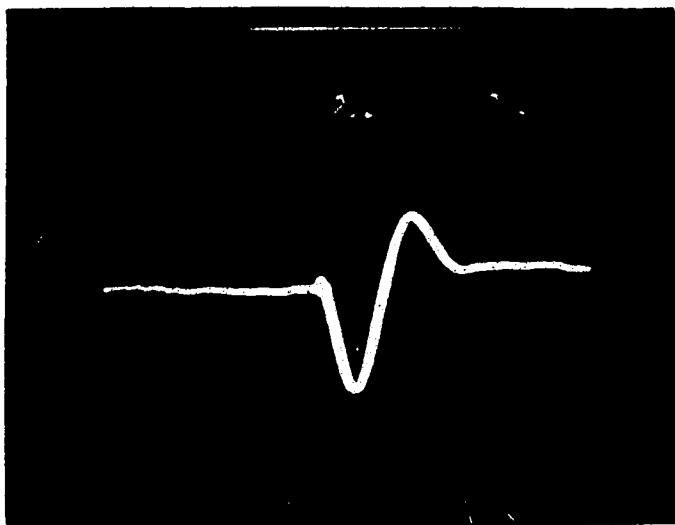


Plate 2 Current Waveform for the $50\mu\text{s}$ Spark

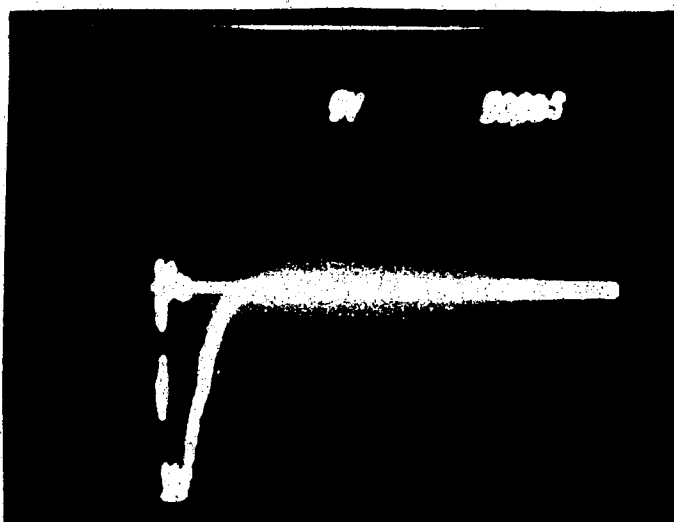


Plate 3 Typical Current Waveform for the Fast Sparks

the spark gap.

For the three other sparks the fifty microsecond discharge was used as a trigger for the three electrode gap in the high voltage fast discharge supply [Fig.7]. In the fast supply a twenty-seven hundred picofarad capacitor was charged to twenty-seven kilovolts to store one joule, and to twenty-one kilovolts to store six-tenths of a joule. A five hundred and seventy picofarad capacitor was charged to twenty kilovolts to store one-tenth of a joule. The three electrode gap was made up of two steel hemispheres separated by air. One hemisphere was grounded and the other was charged to the storage voltage of the capacitor. The slow power supply fired a plasma jet into the space between the two electrodes and the plasma allowed the current to flow from one hemisphere to the other. The capacitor, charged to a large negative voltage and grounded on the other side by a ten megohm resistor, is suddenly grounded on the negative side by the three electrode gap. Since the voltage across a capacitor can not change instantaneously, the previously grounded side jumps to a positive voltage equal to the negative voltage to which the other plate has been charged. This high voltage breaks down the air in the spark gap and the

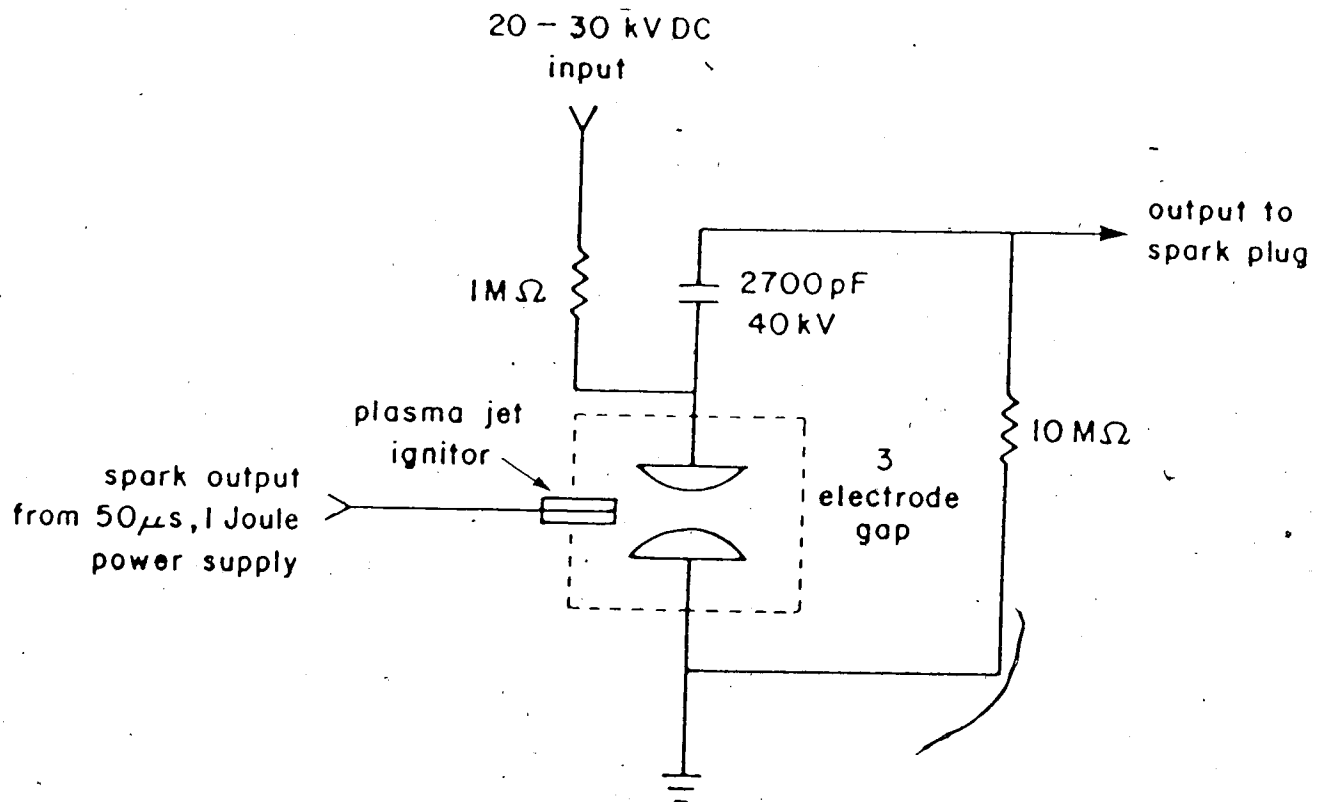


Figure 7 Fast Discharge Power Supply

current flows across the spark gap in the test cell. The three sparks generated by this supply had durations of from five hundred to eight hundred nanoseconds. A current waveform typical of the submicrosecond sparks is shown in Plate 3. Spark duration was measured using a current transformer (Pearson Electronics No. 1025). The spark duration was recorded as the time required for the current to drop to zero.

4.2 Data Collection

The steel test cell was flushed for ten seconds by a mixture of known portions of methane and air, and the turbulence was allowed ten seconds to subside. A spark initiated combustion, and the position of the resulting flame was recorded and digitized by the SP 2000 [Plate 4]. Three trials were averaged to remove some scatter from the results. This data is summarized in Figures 8, 9 and 10.

Four energies and durations were used with three different fuel-air ratios. The stoichiometric mixture for methane in air is nine and one-half percent by volume; tests were done at six, eight and nine and one-half percent. It is apparent from the graphs that for these three mixtures the one joule, eight hundred nanosecond

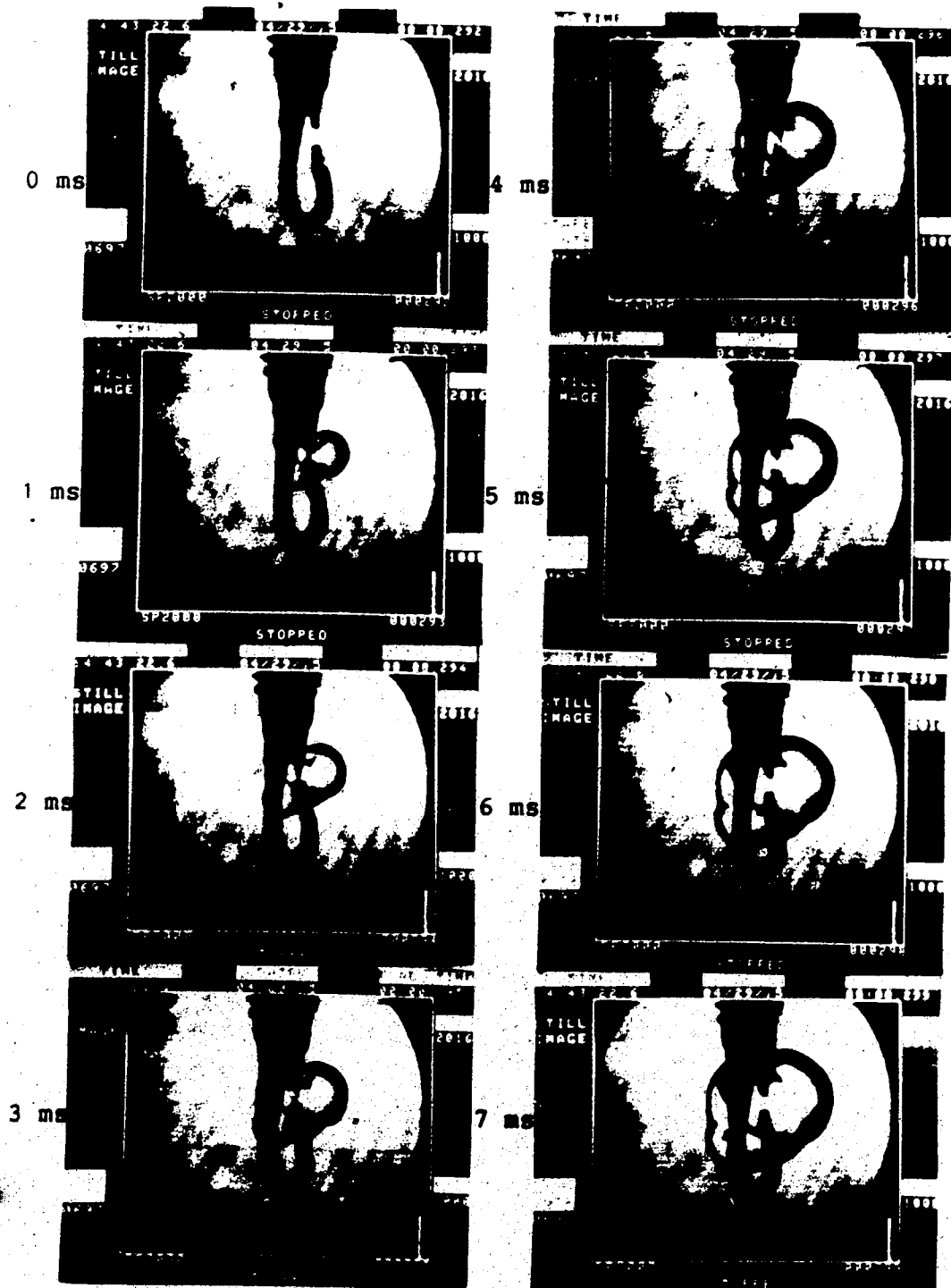


Plate 4 Typical Series of Flame Growth Photographs
 50 μ s, 1 J; $\lambda = 1.0$.

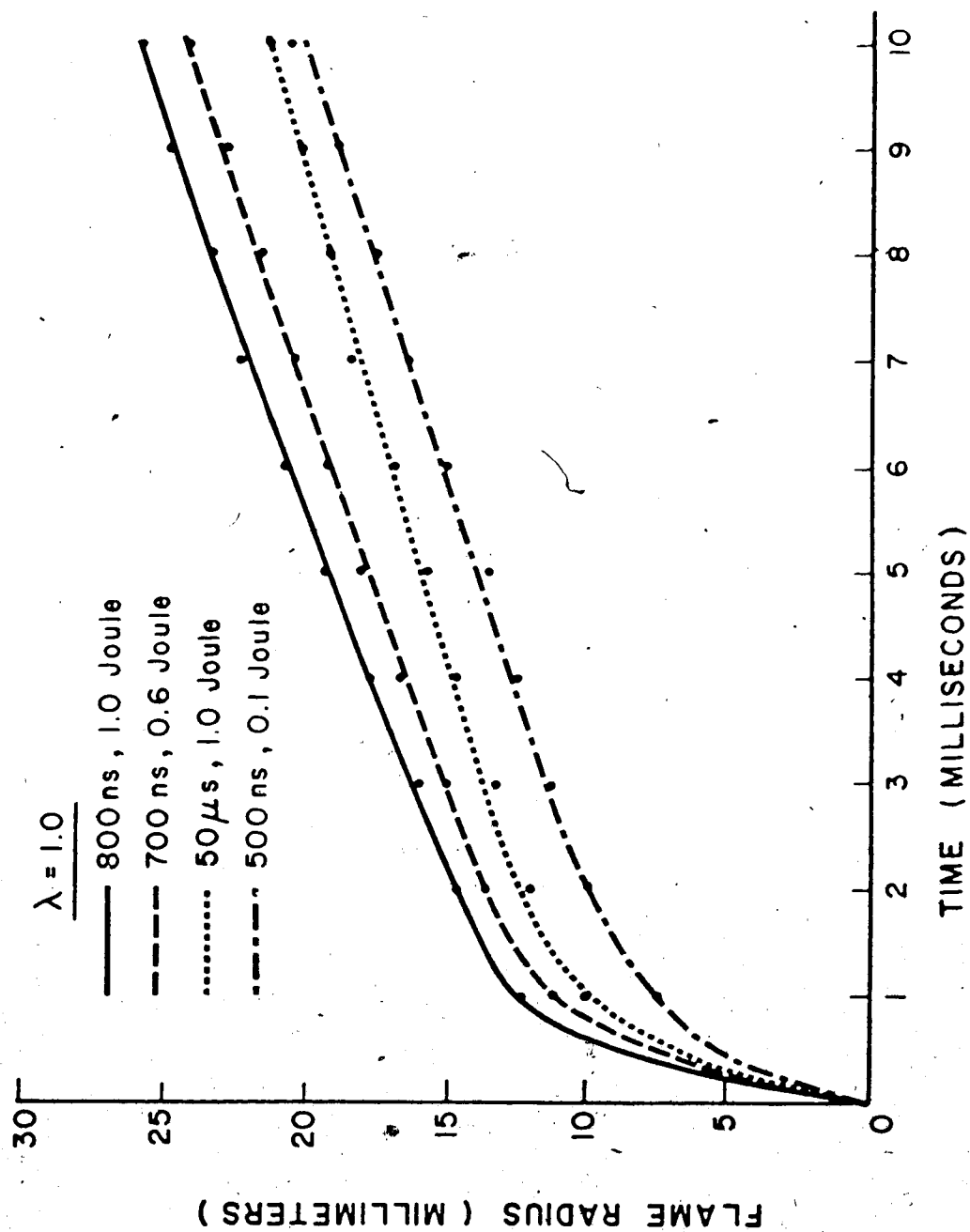


Figure 8 Effect of Spark Source on Flame Front Travel $\lambda = 1.0$

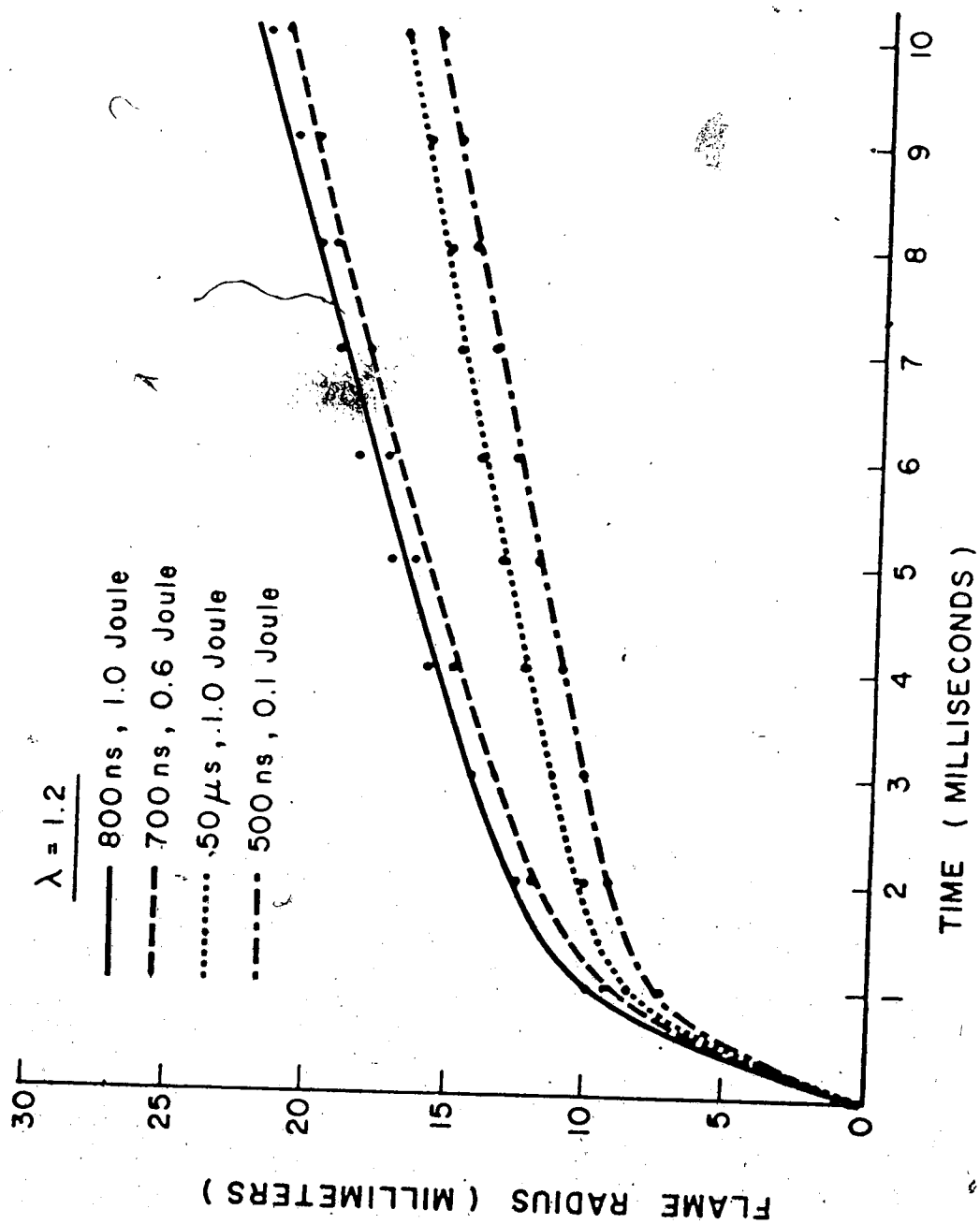


Figure 9 Effect of Spark Source on Flame Front Travel $\lambda = 1.2$

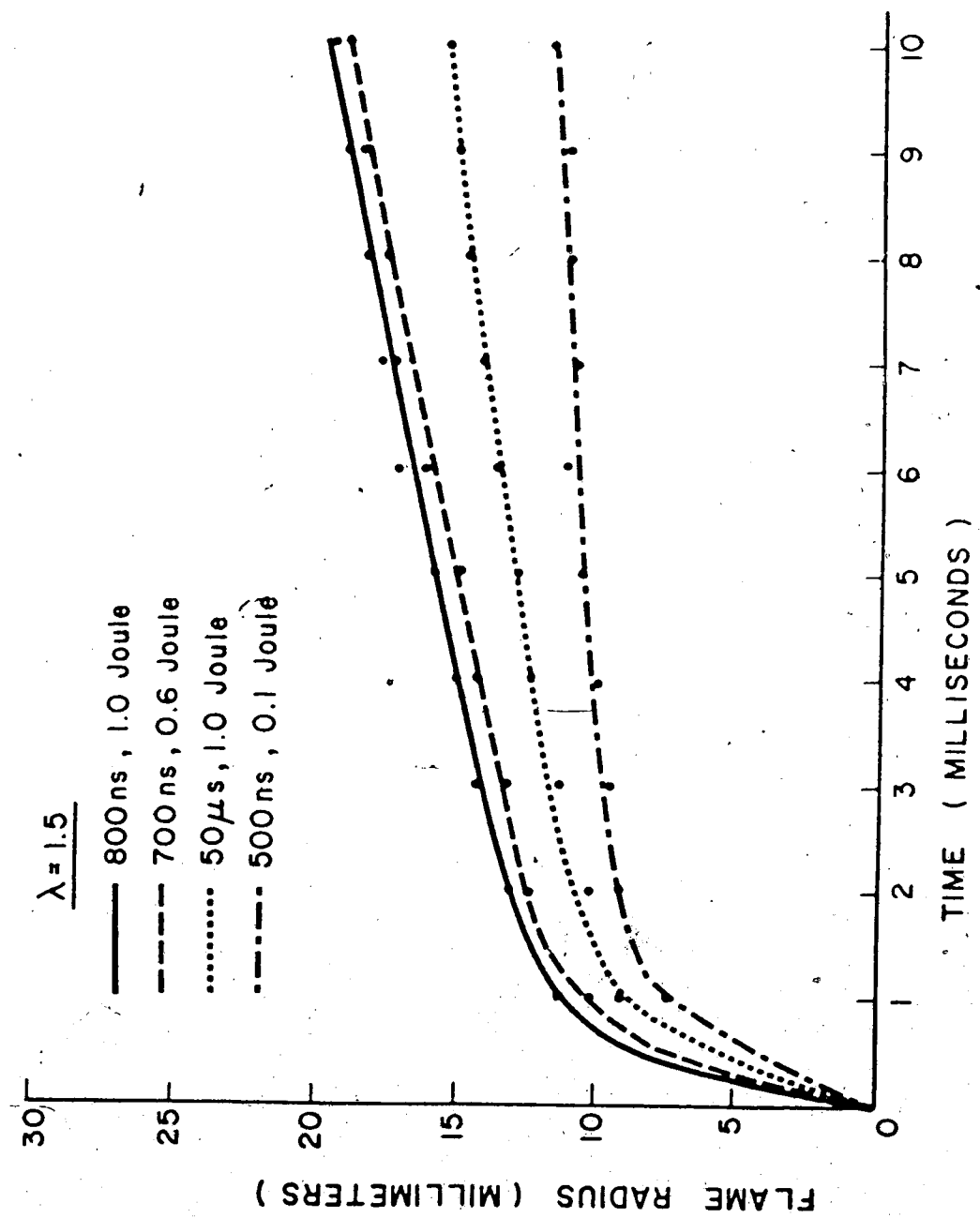


Figure 10 Effect of Spark Source on Flame Front Travel $\lambda = 1.5$

spark ignites a much larger flame kernel. Reducing the energy of the fast spark by forty percent made only an eight percent difference in the flame travel, in the first ten milliseconds, in the stoichiometric mixture. This proves that the duration of the spark is more significant than the energy released when the energy is well above the minimum ignition energy. Studies of very short duration sparks show that the minimum ignition energy is increased from its normal value of 330 μJ for methane at $\lambda = 1.0$ (Ziegler, et al, 1984). Table 2 shows the variation of flame travel for the three submicrosecond sparks in three mixture ratios as compared to the fifty microsecond, one joule spark.

For all three mixtures the flame ignited by the short duration spark of the same energy burned approximately double the volume of fuel during the first five milliseconds [Table 3]. Five milliseconds was the period chosen for numerical examples, but the trends are the same at ten milliseconds as well. An internal combustion engine would require ten milliseconds for the power stroke at three thousand rpm and only five milliseconds at six thousand rpm. This table also shows that the short duration spark which is equal in effectiveness to the one

TABLE 2

FLAME TRAVEL IN 5 MS COMPARED TO THE ONE JOULE, 50 μ s SPARK

Mixture Strength	Spark Characteristics		
	1 J, 800 ns	0.6 J, 700 ns	0.1 J, 500 ns
$\lambda=1.0$	123 %	114 %	89 %
$\lambda=1.2$	127 %	122 %	92 %
$\lambda=1.5$	124 %	118 %	83 %

TABLE 3

VOLUME BURNING IN 5 MS COMPARED TO THE ONE JOULE, 50 μ s SPARK

Mixture Strength	Spark Characteristics		
	1 J, 800 ns	0.6 J, 700 ns	0.1 J, 500 ns
$\lambda=1.0$	186 %	148 %	70 %
$\lambda=1.2$	205 %	182 %	78 %
$\lambda=1.5$	191 %	164 %	57 %

joule, fifty microsecond spark should have a stored energy of about three-tenths of a joule, and a duration of six hundred nanoseconds.

By varying the mixture ratio and using a fixed spark the effect of the mixture was investigated. From Table 4 it can be seen that the effect of the spark duration on flame travel is only slightly dependent on the mixture

TABLE 4

VARIATION OF FLAME TRAVEL WITH MIXTURE RATIO

Duration (Nanoseconds)	Energy (Joules)	$\frac{\lambda=1.2}{\lambda=1.0}$ (%)	$\frac{\lambda=1.5}{\lambda=1.0}$ (%)
50,000	1.0	85	82
800	1.0	88	83
700	0.6	91	85
500	0.1	88	77

being ignited. The difference between sparks igniting $\lambda = 1.0$ and $\lambda = 1.2$ is within six percent and between $\lambda = 1.0$ and $\lambda = 1.5$ the difference is eight percent. Since the data varied from shot to shot by up to twelve percent at $\lambda = 1.5$ it seems that the mixture does not play an important role in the rate of discharge effect. Since the data varied from shot to shot by up to twelve percent at $\lambda = 1.5$ it seems that the mixture does not play an important role in the rate of discharge effect.

5. Spark Thermal Efficiency and Interferometry

5.1 Thermal Efficiency

The apparent combustion enhancement by the short duration spark is due to several processes working together. The efficiency of the fast spark was found to be twice that of the slower, fifty microsecond discharge [Table 5]. To determine the efficiency, the spark gap was discharged in a closed cell with a volume of seventeen cubic centimeters. A piezoelectric probe (Celesco Transducer Products, LD-25) was used to measure the transient pressure rise in the cell. Piezo probe calibration with known pressure transients showed good agreement with the manufacturer's data of thirty-five picocoulombs per pound per square inch. The electrical output from the probe was shunted by a capacitor much larger than the capacitance of the probe and was fed through a one kilohertz low pass filter before the results were displayed and stored on an oscilloscope [Plate 5]. Thermal energy added to the gas (E) in the cell produces a temperature rise ΔT :

$$\Delta T = \frac{T_0 \Delta P}{P_0} = \frac{E}{\rho V C_v}$$

TABLE 5
SPARK EFFICIENCIES

Energy (Joules)	Duration (Nanoseconds)	Efficiency (%)
1.0	50,000	4
1.0	800	8
0.6	700	7
0.1	500	12

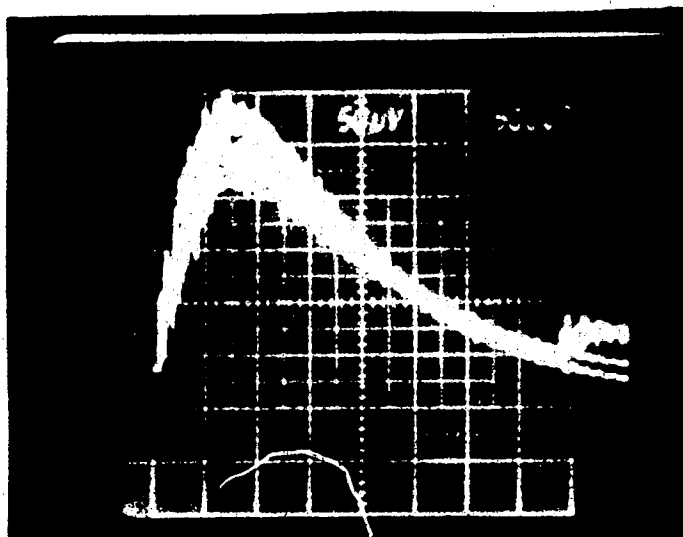


Plate 5 Typical Efficiency Test Output

where ρ is the gas density, C_v is the constant volume specific heat, V is the test cell volume, T_0 is the initial temperature and P_0 is the initial pressure (Smy, et al, 1983). From the general gas law:

$$\frac{P_1 V_1}{T_1} = \frac{P_2 V_2}{T_2}$$

it is known that a temperature rise in a constant volume will produce a proportional rise in pressure. The piezoelectric probe will measure the pressure rise and from this the corresponding temperature rise can be calculated.

To remove the effect of thermal efficiency from the tests, the storage voltage of the fast spark was lowered to reduce the stored energy until the pressure measurements showed the same thermal energy being dumped into the cell. This occurred at a storage voltage of twenty-one kilovolts for an energy of six-tenths of a joule which discharged in seven hundred nanoseconds.

When the 0.6 J, 700 ns spark was compared to the 1.0 J, 800 ns spark, the difference in flame travel was found to be between four and eight percent. The reduction of energy input by forty percent did not seriously reduce the

flame travel enhancement of the fast discharge.

The low efficiency of these spark sources for the transfer of stored electrical energy to thermal energy in the gas lies in the impedance mismatch between the source and load. The arc voltage in the spark gap is fixed by the arc length and the arc current and is usually less than two hundred volts. Source voltages varied from one to twenty-seven kilovolts. Most of the voltage in the discharge is sustained in the power supply, typically sixty to ninety percent, and most of this energy is lost as heat in the circuit outside the arc.

Using the results of Smy et al (1983) where the capacitor, (C) was charged to an initial voltage (V_0) and the arc voltage (V) was taken to be 120 V, the calculated efficiencies of the sparks used here do not agree with the theory. With a stored energy equal to

$$E_S = \frac{1}{2} C V_0^2$$

and an energy dissipated in the gas of

$$E_E = C V V_0$$

the efficiency was given by:

$$\epsilon \approx \frac{C V_0 (120)}{1/2 C V_0^2} = \frac{240}{V_0}.$$

When the voltage data are substituted into the efficiency calculations of Smy, et al the results do not agree with the measured efficiencies. This suggests that there are other factors governing the efficiencies of spark plugs, one of which is the rate of discharge. As the time required to discharge the energy is reduced, more of the energy is fed to the plug when the pressure in the spark gap is still very high (200 bar) and the arc voltage is still elevated. Maly and Vogel (1979) suggest that the arc voltage in the first ten nanoseconds could be as high as fifteen kilovolts. The energy losses in the twenty kilovolt supply would be reduced by seventy-five percent during the stage where both arc voltage and supply voltage are so close in value. The fifteen kilovolt arc would take seventy-five percent of the available energy while the 120 V arc would receive only 0.6 percent.

Thus, the efficiency calculation is probably not valid for submicrosecond sparks, since a large part of the energy is transferred with high efficiency during the high arc voltage early stages of the arc. Longer duration sparks transfer only a small fraction of their energy in

the first ten nanoseconds, so the extra efficiency is swamped by the rest of the discharge at low efficiency.

For example, if the elevated arc voltage provides a ninety percent efficiency for fifty nanoseconds and the 120 V arc voltage provides 1.2 % efficiency for the rest of the twenty kilovolt spark, the one joule, five hundred nanosecond spark should show an efficiency of ten percent. This agrees with the experimental value, and supports the theory that the first tens of nanoseconds allow much more efficient transfer of energy to the gas. A logical extension to this work would be to build and experiment with a power supply with a pulse duration of less than one hundred nanoseconds to investigate the efficiency of even shorter duration sparks.

The large energies used for these experiments result in significant erosion of the electrodes. Erosion is related to the amount of charge which flows through the spark gap (Smy et al, 1983). The fifty microsecond spark used 2×10^{-3} C while the eight hundred nanosecond spark used 7.3×10^{-5} C. The large (30X) difference in charge flow should result in a significant reduction in erosion for the eight hundred nanosecond spark. Therefore, the shorter duration spark has three major advantages: better

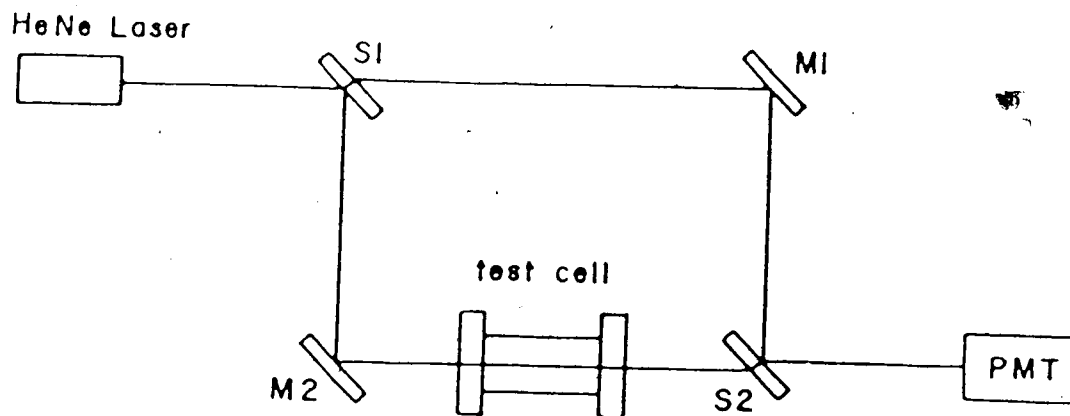
flame speeds, more efficiency and less erosion of the electrodes.

5.2 Interferometry

The test cell for combustion was originally built as a constant volume bomb. Since the measurements for this experiment were complete by the time ten milliseconds had elapsed, it was assumed that any pressure rise in the test cell would not significantly affect the flame speed.

Interferometry was used to measure the pressure rise in the test cell. A Mach-Zehnder interferometer was aimed through the test cell at a point approximately five centimeters from the spark plug (AC Delco 44XLS)[Fig.11]. The Mach-Zehnder set up splits a laser beam into two paths; one through the test cell and the other around the outside of the cell. The two beams are then recombined and produce a fringe shift proportional to the difference in the optical path length of the two beams. The fringe pattern falls on a photomultiplier tube and the output is displayed on an oscilloscope (Bradley, 1962)[Fig.12].

A change in gas density in the test cell will alter the refractive index and this will change the optical path length. Specifically, an increased pressure in the test



M1 and M2 - front surface mirrors
 S1 and S2 - semisilvered optical flats

Figure 11 Mach-Zehnder Interferometer

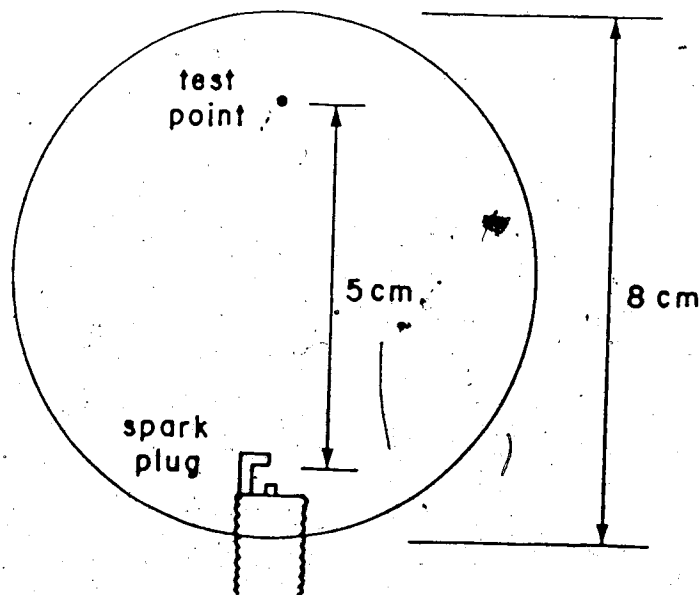


Figure 12 Test Cell Layout for Interferometry

cell will lengthen the optical path of the laser beam which traverses it. A change in density ($\Delta\rho$) of the gas changes the refractive index (Δn) and therefore the optical path (L) by:

$$K L \Delta\rho = \Delta n L = S \lambda.$$

K is the Gladstone-Dale constant $\frac{n-1}{\rho}$, (0.226 for Air), S is the number of fringe shifts and λ is the wavelength of the light used (Bradley, 1962). Another use for the interferometer was to measure the pressure rise in the later stages of combustion. As more fuel is burned the pressure increases and the number of fringe shifts allow the calculation of the pressure rise. However, when the flame front reaches the laser beam, schlieren bending occurs and the fringe shifts abruptly cease. The number of fringes prior to the schlieren bending indicate the amount of fuel which has been burned by the flame when it has reached a known volume [Plate 6].

It was thought that the fast discharge might move the flame front faster because less complete combustion was occurring, indicating a more corrugated and porous flame. However, interferometry showed that the fast discharge

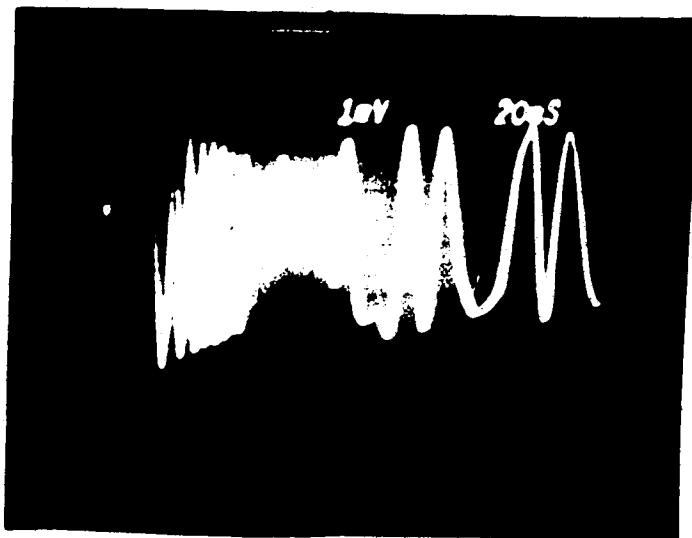


Plate 6 Oscilloscope Output From Interferometer

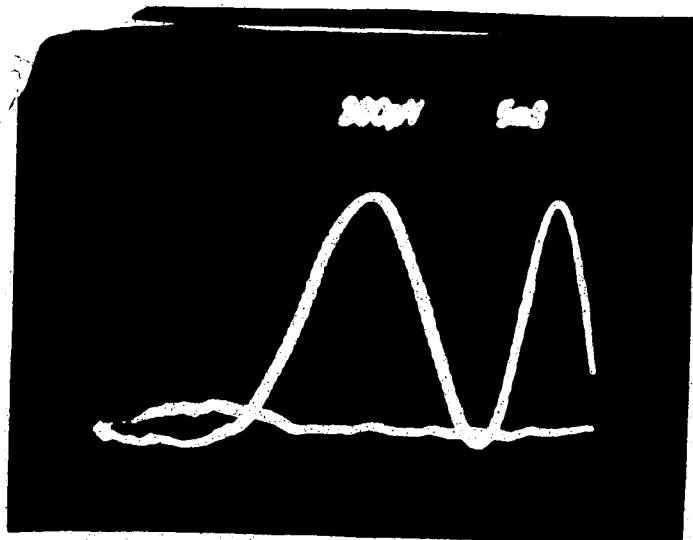


Plate 7 Oscilloscope Output From Interferometer Showing
Little Pressure Rise During the First Ten Milliseconds

()

produced a higher pressure rise and also moved the flame front faster across the cell. This suggests that the fast discharge increases the rate of combustion behind the flame front in addition to spreading the flame faster. Both of these effects would act to complete combustion much sooner when the fuel is ignited by the fast discharge spark. When the combustible mixture was ignited, the fringe shift displayed by the interferometer showed no appreciable pressure rise for the first ten milliseconds, so the data could be treated as a flame in free air [Plate 7].

6. Summary

A schlieren system using a high speed video camera is described which allows the recording of flame kernel development at speeds of up to twelve thousand frames per second. The images were stored on one-half inch recording tape and each frame was illuminated for only one hundred nanoseconds to provide sharp images, including those of the shock waves produced by the electric discharge.

Photographs of the flame kernels in three mixtures of air and methane show a definite improvement when ignition is achieved by short duration sparks. Flame kernels resulting from ignition by short duration sparks were more turbulent and expanded faster than flame kernels ignited by longer duration sparks of the same energy. When the spark sources were compared in air the short duration spark created a finely turbulent puff which travelled nine millimeters in the first millisecond [Plate 8], whereas the slower discharge produced a smooth, spherical puff which travelled only six millimeters in the same amount of time [Plate 9].

Momentum due to the pressure created by the arc and the heat gradient is responsible for the movement of the puff away from the electrodes. These experiments showed

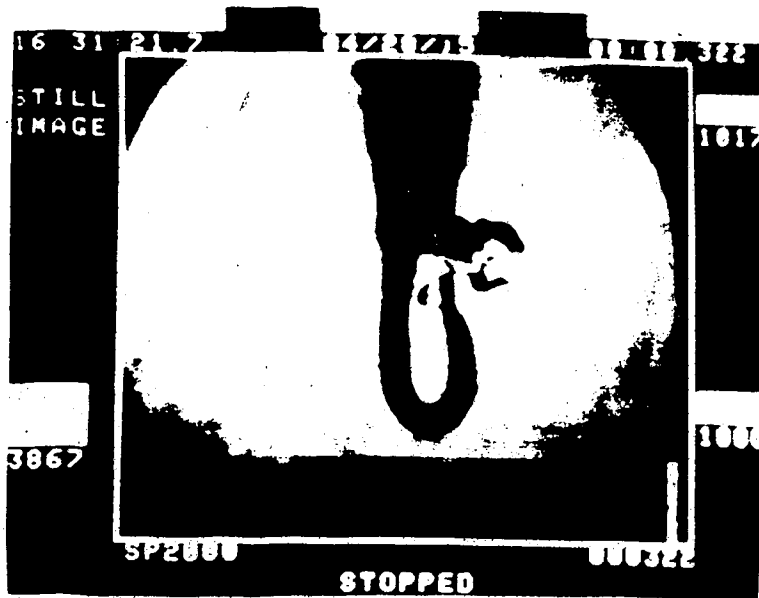


Plate 8 Fast Discharge Flame Kernel; $t=1$ ms.

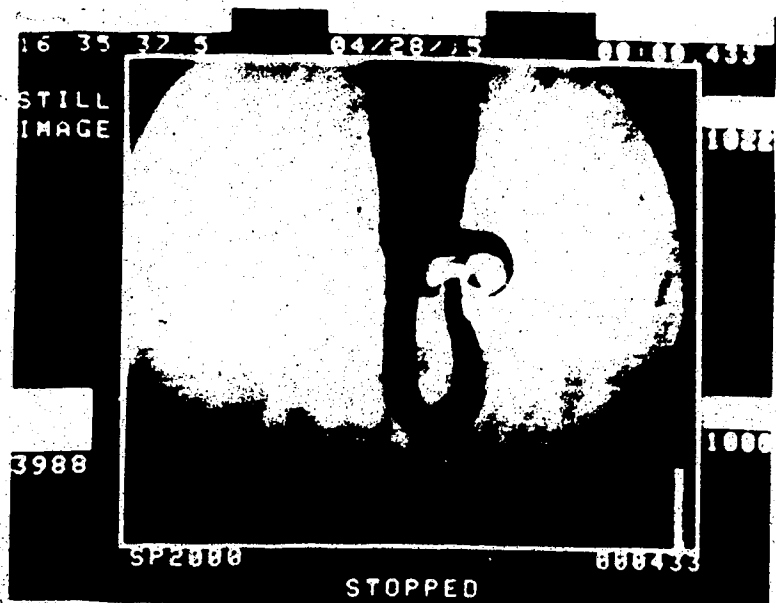


Plate 9 Slow Discharge Flame Kernel; $t=1$ ms.

that the fast discharge is able to deposit more thermal energy in the gas. The fast discharge created a more turbulent puff which would help to increase the flame speed, since a wrinkled laminar flame burns faster than a smooth laminar flame due to the increased surface area. The turbulence would raise the minimum ignition energy, which would explain the behavior of the 0.1 joule, five hundred nanosecond spark in the $\lambda = 1.5$ case [Table 4]. The 0.1 joule spark was able to ignite the gas, but there was a longer ignition delay. Probably, while the turbulence was significant the flame was barely able to sustain itself and as the turbulence died away the flame was able to become established [Fig.10].

The effect of spark efficiency in the test cell was investigated to support the conclusion that faster discharge sparks are more efficient at changing the stored electrical energy to thermal energy in the gas. For stored energies near one joule the energy deposited in the gas is not as important as the rate at which the energy is added. A very short spark duration builds up a steep temperature gradient which upsets the simple theory of energy balance in the flame kernel (Maly, Saggau, Wagner and Zeigler, 1983).

Maly, et al, suggest that the energy gained by the flame kernel from chemical reactions must exceed the energy lost through the surface of the flame. If, however, a large surplus of energy exists in the flame kernel, as in the case of the fast discharge, the energy balance can be biased towards an energy losing situation. For a time determined by the flame kernel temperature the flame may travel at an increased rate, gaining volume at the expense of energy. As the temperature is reduced by spreading the energy over a larger volume the flame must slow down and proceed at the normal flame speed for the mixture it is burning. Therefore the flame is given a head start for the first few milliseconds. It finally reaches the same flame speed as a flame ignited by any other means. This can be seen in Figures 8, 9 and 10.

Laser interferometry showed that the pressure in the test cell did not rise appreciably in the first ten milliseconds. Since all of the measurements were complete by this time no corrections for changing flame speed were required and this experiment could be treated as if it had occurred in open air.

The schlieren camera described here should prove useful in future flame studies, and the data on fast

discharge spark ignition will, hopefully, lead to a better understanding of spark ignition.

References

- Bradley, J. N. *Shock Waves in Chemistry and Physics*. London: Methuen and Co., 1962.
- Clarke, C. F., M. C. Hales, J. Walters, H. H. Nathan, A. Laughton. "Low Coherence Laser for Analog Systems Use" *Laser Focus / Electro Optics*. June 1985, p. 102.
- Dainty, J. C. "Stellar Speckle Interferometry." *Laser Speckle and Related Phenomena*. Berlin: Springer-Verlag, pp. 267-268, 1984.
- Fabian, M. E. *Semiconductor Laser Diodes; A Users Handbook*. Electrochemical Publications Ltd., 1981.
- Gettel, L. E. and K. C. Tsai. "The Effect of Enhanced Ignition on the Burning Characteristics of Methane Air Mixtures" *Combustion and Flame*. Vol. 54 pp. 183-193, 1983.
- Keck, J. C. "Turbulent Flame Structure and Speed in Spark Ignition Engines." *Nineteenth Symposium (International) on Combustion*. pp. 1451-1466, 1982.
- Lewis, B., G. von Elbe. *Combustion, Flames and Explosions of Gases* Academic Press, second edition, 1961.
- Maly, R. "Ignition Model for Spark Discharges and the Early Phase of Flame Front Growth." *Eighteenth Symposium (International) on Combustion*, Pittsburgh: The Combustion Institute pp. 1747-1754, 1980.
- Maly, R. and M. Vogel. "Initiation and Propagation of Flame Fronts in Lean CH_4 - Air Mixtures by the Three Modes of the Ignition Spark." *Seventeenth Symposium (International) on Combustion*. Pittsburgh: The Combustion Institute, pp. 821-31, 1979.
- Maly, R., Saggau, B., Wagner, E., and Zeigler, G. *Prospects of Ignition Enhancement*. SAE Paper No. 830478, 1983.
- McGeer, P. and E. Durbin editors *Methane: Fuel for the Future* New York: Plenum Press, 1982.
- Obert, E. F. *Internal Combustion Engines* New York: Intext. Educational Publishers, 1973.

Optics Guide 3. Melles-Griot pp. 370 - 373, 1985.

Smy, P. R., R. M. Clements, J. D. Dale, D. J. Simieoni and D. R. Topham. "Efficiency and Erosion Characteristics of Plasma Jet Ignitors." *Journal of Physics D: Applied Physics*. Volume 16 p. 783, 1983.

Webster's Seventh New Collegiate Dictionary. Toronto: Thomas Allen and Son Ltd., 1973.

Weinberg, F. J. *Optics of Flames*. London: Butterworths, 1963.

Wright, J. K. *Shock Tubes* London: Methuen & Co. pp. 40-51, 1961.

Ziegler, F. W., E. P. Wagner and R. R. Maly 'Ignition of Lean Methane-Air Mixtures by High Pressure Glow and Arc Discharges.' *Twentieth Symposium (International) on Combustion*. Pittsburgh: The Combustion Institute, pp. 1817-1824, 1984.